ACS APPLIED MATERIALS & INTERFACES

RESEARCH ARTICLE

www.acsami.org

En Route to White-Light Generation Utilizing Nanocomposites Composed of Ultrasmall CdSe Nanodots and Excited-State Intramolecular Proton Transfer Dyes

Hsin-Chieh Peng,[†] Chia-Cheng Kang,[*,‡] Ming-Ren Liang,[†] Chun-Yen Chen,[†] Alexander Demchenko,[§] Chao-Tsen Chen,[*,†] and Pi-Tai Chou[*,†]

[†]Department of Chemistry, National Taiwan University, 1 Roosevelt Rd., Sec. 4 Taipei 106, Taiwan

[‡]Department of Chemistry, Fu Jen Catholic University, 510 Zhongzheng Rd., Xinzhuang Dist., New Taipei City, 24205, Taiwan

[§]Palladin Institute of Biochemistry, National Academy of Sciences of Ukraine, 9 Leontovicha, Kiev, 01030, Ukraine

Supporting Information

ABSTRACT: One single material that emits white light is of paramount interest for the development of white light-emitting diodes (WLEDs). Here we report a novel nanocomposite, in which a new type of excited-sate intramolecular proton transfer (ESIPT) molecule, namely 5-(1,2-dithiolan-3-yl)-*N*-(2-{[4-(3-hydroxy-4-oxo-4H-chromen-2-yl)phenyl](methyl)amino}ethyl)pentanamide (HF-N-LA), is anchored onto the surface of ultrasmall CdSe quantum dots through dithiol functionality. Authentic white light with a CIE coordinate of (0.33, 0.33) could then be generated by confluence of 440 nm emission from CdSe and 570 nm proton-transfer tautomer emission from HF-N-LA. Moreover, linear color tunability could be achieved simply by altering relative amount of the two species, i.e., number of HF-N-LA onto CdSe, in one single nanocomposite, thus opening an innovative route toward applying nanocrystals in the field of WLEDs.

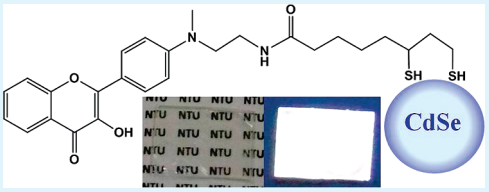

KEYWORDS: quantum dots, CdSe, nanocomposite, excited-sate intramolecular proton transfer (ESIPT), white light generation, light-emitting diodes (LEDs)

INTRODUCTION

Owing to the growing concern of global warming and energy crisis, the demand of searching more efficient devices such as white light-emitting diodes (WLEDs) has become one of the most widely studied subjects in modern scientific and technological fields. Comparing with conventional fluorescent and incandescent lamps, white light-emitting diodes possess higher efficiency and smaller size, thus being capable of not only replacing the traditional light sources but also greatly extending their potential in diverse applications ranging from backlight of flat panel display to vehicle headlamps.[1,2] Although it has been demonstrated that the YAG based WLEDs could serve as a promising material in solid state lighting, they still suffer from low color rendering index as well as the fixed emission wavelength, limiting the versatility in many other aspects. From then on, efforts have been made intensively to explore materials for better performance en route to white light-emitting diodes, for example, the QD-based WLEDs.[3−6]

Zero dimensional II−VI and/or III−V semiconducting nanoparticles (also referred to as "quantum dots") possessing intensive emissions as well as tunable energy gaps[7] have made them applicable in diverse fields such as display,[8] bioimaging,[9] and photovoltaic devices.[10,11] Recently, owing to the advanced progress of developing novel synthetic routes for producing application-oriented semiconducting nanocrystals, a new family of ultrasmall quantum dots (USQDs) has emerged for their nearly uniform size distribution and the corresponding narrower emission bandwidth in comparison with the normal QDs.[12−16] Free from the inhomogeneous broadening that is commonly observed for normal QDs, these cluster-like ultrasmall QDs are thought to be more suitable for fundamental and application-oriented research. Within the category of ultrasmall QDs, those with specific number of atoms and therefore unique band gap absorption as well as emission spectra are also called magic-sized quantum dots.[12,13,16]

Among various approaches, the nanocomposite being able to exhibit multiple emission color in one unit is an intriguing as well as important issue. Comparing with blending different kinds of luminescent materials such as inorganic phosphors, single component with more than one emission color could reduce the complexity in device fabrication, thus offering a more economical strategy toward practical applications. Upon anchoring ligands having designated chromophores, energy transfer may take place between ligands and quantum dots,[17−19] rendering multiple emission colors in one unit possible. In combination with multivalent effects exerted by the strategically designed recognition units (the ligands) on the QDs, molecule/ion sensing and/or imaging nanocomposites have been demonstrated with great sensitivity

Received: February 22, 2011
Accepted: April 27, 2011
Published: May 06, 2011

via ratiometric type of dual or even multiple emissions.[17−19] And yet highly intensive, multiple-emission generation in an entity of nanocomposite awaited to be explored in the application of the white light generation suited for, for example, display.

The requirement of multiple emitting color generation within a single nanocomposite lies in that each emitting color should not quench each other via common deactivation pathways such as energy transfer, electron transfer, or even radiative reabsorption dubbed as trivial energy transfer, etc. For a molecular dyad or even triad composed of, for example, dual emitting fluorophores, one can in theory devise this entity strategically that the lower-lying absorption bands of one emitting fluorophore per se have negligible overlap with emission of the other fluorophore possessing higher energy gap. As such, resonance type of energy transfer is inhibited and the dual emissions virtually have negligible interaction. Similar theory and hence protocol may be applied to triad or higher.[20−22] This requirement, however, is a great challenge in terms of nanocomposite made by, for example, quantum dots, simply because of the quasi-continuous, largely increasing of the absorption toward the higher energy region. Thus, attempts to use QDs as the long wavelength emissive candidate hamper any design of the second-higher-energy fluorophore. Although reverse of emission order might work, it is not trivial at all to choose suitable fluorophores for which the absorption bands have negligible overlap with emission bands of QDs. Particularly, for the latter case, the close proximity between the band edge absorption and the emission for QDs also implies negligible absorption required for the designed fluorophore.

As an alternative, one facile approach is to combine QDs and organic fluorophores so that both possess similar lowest lying energy gaps. Upon simultaneous excitation, the designated fluorophore undergoes ultrafast chemical event in the excited state, resulting in a large Stokes' shifted emission that is free from QDs interference. One prompt proposal may rely on the excited-state charge transfer molecules, which undergo fast solvent-dependent relaxation, giving a large Stokes's shifted emission in solution. Unfortunately, the hindrance of solvent rotation in the highly viscous or even rigid media may impede their practical application.

To our viewpoint, a case in point should be ascribed to those molecules exhibiting excited-sate intramolecular proton transfer (ESIPT). The ESIPT reaction generally requires hydrogen-bonding formation between the vicinal proton donor (hydroxyl or amino proton) and the acceptor groups (carbonyl oxygen or pyridyl nitrogen) that exist in the molecule (or complex) per se. Upon electronic excitation, proton transfer takes place along the potential energy surface (PES) associated with hydrogen bond, forming a proton-transfer tautomer, which, in theory, possesses significant differences in both the structure and the electronic configuration from its corresponding normal species, resulting in a large Stokes' shifted proton-transfer tautomer fluorescence. For ESIPT molecules with strong hydrogen bonding strength, the coupling of PES between the reactant (normal species) and the product (the proton transfer tautomer species) is large and hence ESIPT is commonly barrierless or modulated by the vibrational motions associated with hydrogen bonds;[23−25] its time scale is generally $\ll$1 ps in both nonpolar solvents and the solid state. On this basis, one can thus select QDs encapsulated by ESIPT molecules, in which QDs is designed (via tuning size) to have only slightly lower energy gap than that of the ESIPT molecules. Upon excitation, regular band gap emission is observed for QDs, whereas the ligand fluorophore exhibits proton-transfer emission at much longer wavelengths. Because of the ultrafast rate of ESIPT, the anomalously large Stokes' shifted proton-transfer emission should be free from QDs interference, generating an ideal dual emission, for which each possesses its own emitting character. What is more, the intensity ratio for QDs versus ESIPT molecules can be fine-tuned via the number of ligands anchoring on QDs. As elaborated in the following section, white-light generation can thus be achieved through ingenious design of QDs and ESIPT fluorophores. In this study, utilization of ultrasmall CdSe QDs in white emissive nanocomposites takes the advantage of the high surface-to-volume ratio, hence the homogeneity of nanocomposites could be easily controlled by incorporating relatively small amount of organic molecules. Furthermore, the overall small size highly increases the feasibility of these white emissive nanocomposites in different applications.

EXPERIMENTAL SECTION

Synthesis of the HF-N-LA Molecule. The synthetic route of HF-N-LA is depicted in Scheme 1, and details of the synthetic procedures as well as structural characterizations are described as follows.[26,27]

2-[Methyl(phenyl)amino]ethan-1-ol (1). 2-Bromoethanol (4.9 mL, 69.01 mmol) was added to a solution of *N*-methylaniline (5.0 mL, 46.06 mmol) and sodium hydroxide (1.840 g, 46.06 mmol) in the cosolvents of acetone (15 mL) and water (8 mL) at room temperature and the reaction mixture was stirred for 12 h at 70 °C. The resulting mixture was poured into water (100 mL) and extracted with ethyl acetate (4 × 20 mL). The combined organic layers were washed with brine (10 mL), dried over $MgSO_4$, filtered, and concentrated under reduced pressure. The residue was purified by flash column chromatography on silica gel with ethyl acetate−hexane (1:4) as an eluent to yield 2.741 g (18.13 mmol) of **1** as a light yellow oil in 39%. TLC (ethyl acetate/hexane (1:4)) R_f = 0.13. IR (KBr) 3417 (ν OH) cm^{-1}. ^1H NMR (400 MHz, CDCl3) δ 7.21 (dd, J = 8.8, 7.2 Hz, 2H), 6.77 (d, J = 8.8 Hz, 2H), 6.72 (t, J = 7.2 Hz, 1H), 3.77 (t, J = 5.6 Hz, 2H), 3.44 (t, J = 5.6 Hz, 2H), 2.93 (s, 3H). ^{13}C NMR (100 MHz, CDCl3) δ 149.9, 129.0, 117.1, 112.9, 60.1, 55.5, 38.8. ESI-HRMS: calcd for $C_9H_{14}NO$ ($[M+H]^+$), 152.1070; found, 152.1074.

***N*-(2-Azidoethyl)-*N*-methylaniline (2).** To a solution of **1** (2.657 g, 17.57 mmol) and triethylamine (3.9 mL, 28.16 mmol) in anhydrous dichloromethane (26 mL) was added methanesulfonyl chloride (2.2 mL, 28.16 mmol) at 0 °C, and the solution was then warmed to room temperature followed by stirring for 4 h. The resulting mixture was filtered through a pad of Celite, washed with dichloromethane (20 mL), and concentrated under reduced pressure to afford crude methanesulfonate. Sodium azide (2.280 g, 35.07 mmol) was added to a solution of crude methanesulfonate in *N*,*N*-dimethylformamide (20 mL) at room temperature and the reaction mixture was stirred for 12 h at 80 °C. The resulting mixture was poured into water (200 mL) and extracted with ether (4 × 20 mL). The combined organic layers were washed with brine (20 mL), dried over $MgSO_4$, filtered, and concentrated under reduced pressure. The residue was purified by flash column chromatography on silica gel with ethyl acetate−hexane (1:40) as an eluent to yield 1.950 g (11.06 mmol) of **2** as a pale yellow oil in 63%.TLC (ethyl acetate/hexane (1:40)) R_f = 0.35; IR (KBr) 2098 (ν N_3) cm^{-1}. ^1H NMR (400 MHz, $CDCl_3$) δ 7.30−7.22 (m, 3H), 6.78−6.72 (m, 2H), 3.56 (t, J = 6.0 Hz, 2H), 3.47 (t, J = 6 Hz, 2H), 3.02 (s, 3H). ^{13}C NMR (100 MHz, $CDCl_3$) δ 148.3, 129.2, 116.9, 112.2, 52.1, 48.9, 38.9. ESI-HRMS: calcd for $C_9H_{13}N_4$ ($[M+H]^+$), 177.1135; found, 177.1140.

4-[(2-Azidoethyl)(methyl)amino]benzaldehyde (3). Phosphoryl chloride (1.6 mL, 16.63 mmol) was added dropwise to anhydrous *N*,*N*-dimethylformamide (3.3 mL) at 0 °C. After stirring at 0 °C for

Scheme 1. (A) Synthetic Routes and Structure of HF-N-LA and (B) Excited-State Intramolecular Proton Transfer (ESIPT) Reaction in HF-N-LA

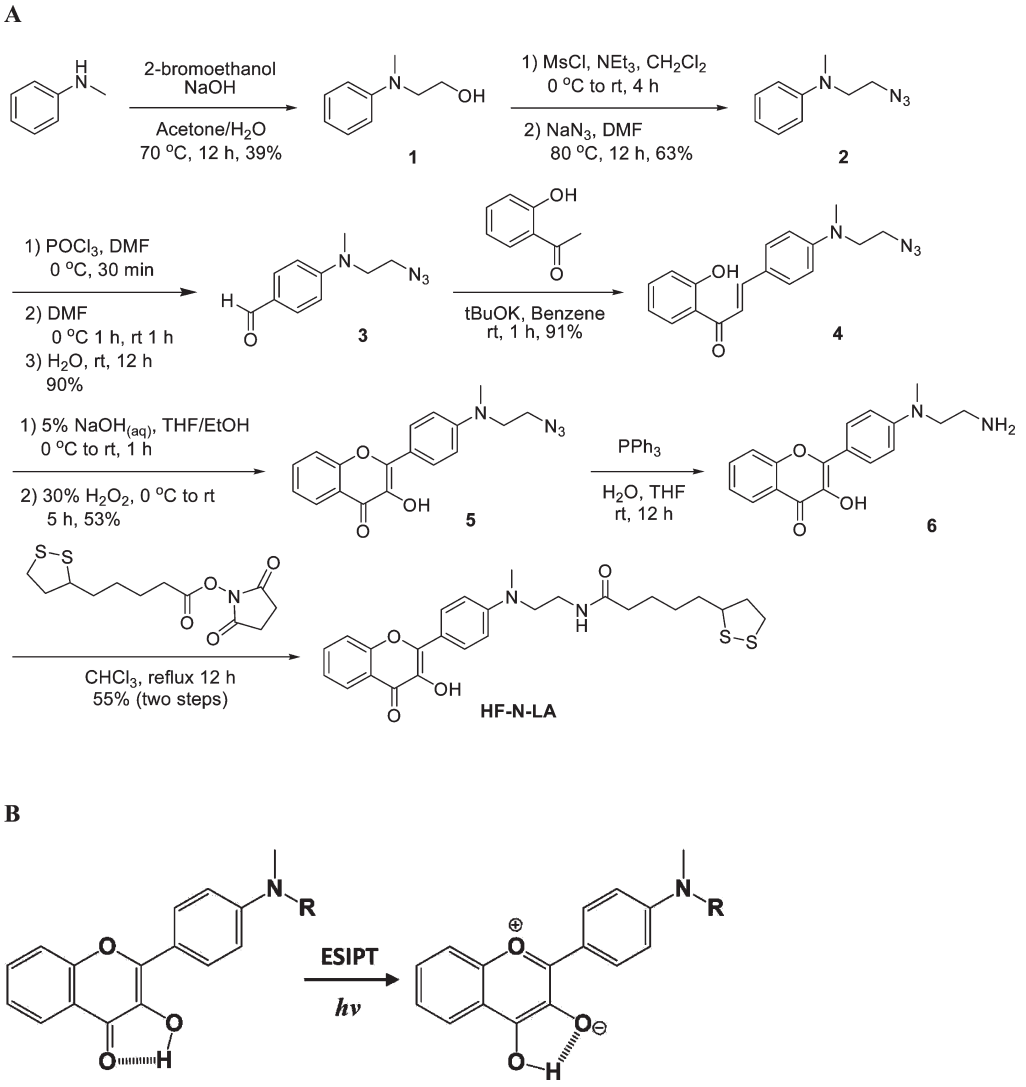

30 min, a solution of **2** (1.950 g, 11.06 mmol) in anhydrous *N*, *N*-dimethylformamide (8.3 mL) was added to the reaction mixture, and then stirred at room temperature for 1 h. The resulting mixture was quenched by water (80 mL) and stirred at room temperature for 12 h. The reaction mixture was then extracted with dichloromethane (4 × 30 mL). The combined organic layers were washed with brine (10 mL), dried over $MgSO_4$, filtered, and concentrated under reduced pressure. The residue was purified by flash column chromatography on silica gel with ethyl acetate−hexane (1:4) as an eluent to yield 2.035 g (9.96 mmol) of **3** as a pale yellow oil in 90%. TLC (ethyl acetate/hexane (1:4)) R_f = 0.19. IR (KBr) 2736 (ν C(=O)H) cm^{-1}, 2098 (ν N_3) cm^{-1}, 1667 (ν C=O) cm^{-1}. ^{1}H NMR (400 MHz, $CDCl_3$) δ 9.69 (s, 1H), 7.69 (d, *J* = 8.4 Hz, 2H), 6.70 (d, *J* = 8.4 Hz, 2H), 3.59 (t, *J* = 6.0 Hz, 2H), 3.47 (t, *J* = 6 Hz, 2H), 3.07 (s, 3H). ^{13}C NMR (100 MHz, $CDCl_3$) δ 189.8, 152.6, 131.8, 125.6, 110.9, 51.3, 48.7, 38.9. ESI-HRMS: calcd for $C_{10}H_{13}N_4O$ ($[M+H]^+$), 205.1084; found, 205.1094.

(2*E*)-3-{4-[(2-Azidoethyl)(methyl)amino]phenyl}-1-(2-hydroxyphenyl) prop-2-en-1-one (4). **3** (0.313 g, 1.53 mmol) and 2-hydroxyacetophenone (184 μL, 1.53 mmol) in benzene (5 mL) was slowly added potassium *tert*-butoxide (0.343 g, 3.06 mmol), and the reaction mixture was stirred for 1 h at room temperature. The resulting mixture was poured into 1N HCl solution (40 mL) and extracted with dichloromethane (3 × 20 mL). The combined organic layer was washed with brine (10 mL), dried over $MgSO_4$, filtered, and concentrated under reduced pressure. The residue was purified by recrystallization from ethyl acetate to afford 0.447 g (1.39 mmol) of **4** as an orange oil in 91%. TLC (ethyl acetate/hexane (1:3)) R_f = 0.38. IR (KBr) 2097 (ν N_3) cm^{-1}, 1631 (ν C=O) cm^{-1}. ^{1}H NMR (400 MHz, $CDCl_3$) δ 13.11 (s, 1H), 7.90 (dd, *J* = 8.0, 1.6 Hz, 1H), 7.88 (d, *J* = 15.6 Hz, 1H), 7.56 (d, *J* = 8.8 Hz, 2H), 7.47−7.43 (m, 2H), 6.99 (dd, *J* = 8.4, 1.2 Hz, 1H), 6.93−6.89 (m, 1H), 6.71 (d, *J* = 8.8 Hz, 2H), 3.61 (t, J = 6.0 Hz, 2H), 3.49 (t, J = 6.0 Hz, 2H), 3.09 (s, 3H). ^{13}C NMR (100 MHz, $CDCl_3$) δ 193.1, 163.2, 150.4, 145.9, 135.5, 130.7, 129.2, 122.8, 120.1, 118.4, 118.2, 114.6, 111.7, 51.4, 48.8, 38.9. ESI-HRMS: calcd for $C_{18}H_{19}N_4O_2$ ($[M+H]^+$), 323.1503; found, 323.1515.

2-{4-[(2-Azidoethyl)(methyl)amino]phenyl}-3-hydroxy-4H-chromen-4-one (5). To a solution of **4** (447 mg, 1.39 mmol) in the cosolvents of THF (4.6 mL) and ethanol (13.9 mL) was added 5% sodium hydroxide aqueous solution (4.6 mL) at 0 °C, and then warmed up to room temperature in 1 h. To the reaction mixture was added 30% hydrogen peroxide (480 μL) at 0 °C, and the solution was then warmed to room temperature followed by stirring at room temperature for 5 h.

The resulting mixture was poured into 1N HCl solution (20 mL) and extracted with dichloromethane (3 × 10 mL). The combined organic layers were washed with brine (10 mL), dried over $MgSO_4$, filtered, and concentrated under reduced pressure. The residue was purified by recrystallization from ethyl acetate to afford 249 mg (0.74 mmol) of **5** as a yellow solid in 53%. Mp 120−121 °C; TLC (ethyl acetate/hexane (1:3)) R_f = 0.30. IR (KBr) 3282 (ν OH) cm^{-1}, 2097 (ν N_3) cm^{-1}, 1600 (ν C═O) cm^{-1}. ^{1}H NMR (400 MHz, $CDCl_3$) δ 8.20 (dd, J = 7.6, 1.2 Hz, 1H), 8.17 (d, J = 8.8 Hz, 2H), 7.68−7.60 (m, 1H), 7.52 (d, J = 8.4 Hz, 1H), 7.38−7.32 (m, 1H), 7.00−6.92 (bs, 1H), 6.78 (d, J = 8.8 Hz, 2H), 3.62 (t, J = 6.0 Hz, 2H), 3.50 (t, J = 6 Hz, 2H), 3.10 (s, 3H). ^{13}C NMR (100 MHz, $CDCl_3$) δ 172.4, 154.9, 149.4, 146.1, 136.9, 132.8, 129.3, 125.1, 120.7, 118.9, 117.9, 111.4, 51.5, 48.9, 38.9; ESI-HRMS: calcd for $C_{18}H_{17}N_4O_3$ ($[M+H]^+$), 337.1295; found, 337.1305.

5-(1,2-Dithiolan-3-yl)-N-(2-{[4-(3-hydroxy-4-oxo-4H-chromen-2-yl)phenyl](methyl)amino}ethyl)pentanamide (HF-N-LA). Water (73 μL) was added to a solution of **5** (271 mg, 0.81 mmol) and triphenylphosphine (232 mg, 0.89 mmol) in THF (10 mL), and the reaction mixture was stirred at room temperature for 12 h. The resulting mixture was concentrated under reduced pressure, and the yellowish residue was purified by triturating with a large amount of dichloromethane (150 mL) to give crude **6** as a yellow solid, which was taken up in chloroform (10 mL). 2,5-Dioxopyrrolidin-1-yl 5-(1,2-dithiolan-3-yl)pentanoate (322 mg, 1.06 mmol) was added to the aforementioned suspension of crude **6** at room temperature, and the reaction mixture was stirred at 60 °C for 12 h. The resulting mixture was poured into water (40 mL) and extracted with dichloromethane (3 × 20 mL). The combined organic layers were washed with brine (10 mL), dried over $MgSO_4$, filtered, and concentrated under reduced pressure. The residue was purified by column chromatography on silica gel with chloroform-ethyl acetate (7:3) as an eluent to yield 219 mg (0.44 mmol) of **HF-N-LA** as a yellow solid in 55%. Mp 148−149 °C; TLC (chloroform/ethyl acetate (7:3)) R_f = 0.31. IR (KBr) 3440 (ν OH) cm^{-1}, 3307 (ν NH) cm^{-1}, 1629 (ν C═O) cm^{-1}, 1595 (ν C═O) cm^{-1}. ^{1}H NMR (400 MHz, $CDCl_3$) δ 8.18 (dd, J = 8.4, 1.6 Hz, 1H), 8.14 (d, J = 9.2 Hz, 2H), 7.68−7.60 (m, 1H), 7.55−7.50 (m, 1H), 7.38−7.32 (m, 1H), 6.95−6.85 (bs, 1H), 6.81 (d, J = 9.2 Hz, 2H), 5.78 (t, J = 6 Hz, 1H), 3.58 (t, J = 6.8 Hz, 2H), 3.51−3.44 (m, 2H), 3.25−3.00 (m, 2H), 3.04 (s, 3H), 2.45−2.35 (m, 1H), 2.13 (t, J = 7.2 Hz, 2H), 1.80−1.70 (m, 1H), 1.70−1.55 (m, 4H), 1.50−1.35 (m, 2H). ^{13}C NMR (100 MHz, $CDCl_3$) δ 172.9, 172.3, 154.9, 150.2, 146.2, 136.8, 132.8, 129.3, 125.1, 124.1, 120.7, 118.5, 117.9, 111.4, 56.4, 51.2, 40.3, 38.5, 38.4, 37.3, 36.5, 34.7, 29.0, 25.3. ESI-HRMS: calcd for $C_{26}H_{29}N_2O_4S_2$ ($[M-H]^-$) 497.1574; found, 497.1561.

Synthesis of the Ultrasmall CdSe Quantum Dots (USQDs). The synthetic procedure of producing ultrasmall CdSe QDs is adapted from that reported by Riehle et al.[15] Briefly, 0.0257 g (0.2 mmol) of cadmium oxide (CdO, 99.99%, Strem Chemicals) and 0.199 g (0.7 mmol) of stearic acid (>95%, Sigma-Aldrich) were loaded into a 50 mL three-neck flask and heated to 200 °C under continuous flow of Nitrogen gas to form a Cd-stearat mixture. After confirming the CdO was thoroughly converted to Cd-Stearat, judging by the disappearance of the brown color of CdO, the temperature of reaction system was kept for 30 min and then cooled down to room temperature. Then, 2.415 g (10 mmol) of hexadecylamine (HDA, 90%, TCI) and 3.866 g (10 mmol) of tri-*n*-octylphosphine oxide (TOPO, 90%, Sigma-Aldrich) were added into the flask. Subsequently, temperature of the reaction system was raised to 200 °C under N_2 flow to obtain a colorless mixture. After 2 h, the temperature was cooled down to 80 °C. Meanwhile, a selenium injection solution containing 0.016 g (0.2 mmol) of selenium (Se, 99.5%, ACROS) was prepared by dissolving selenium powder in 0.2 mL of tri-*n*-octylphosphine (TOP, >95%, TCI). After being cooled to 80 °C, the selenium injection solution was swiftly injected into the flask, and the reaction system was heated to 100 °C under a continuous N_2 flow for 52 h to obtain the ultrasmall CdSe QDs.

For the purification of the as-prepared USQDs, after 52 h, the temperature was lowered to 35 °C to terminate the reaction. In order to remove the remaining unreacted precursors and surfactants, 10 mL of chloroform was introduced to dissolve the reaction mixture, and precipitate was obtained by adding 10 mL of isopropanol and centrifuged at 9500 rpm for 10 min. The precipitate was washed with chloroform and isopropanol three times and redispersed in toluene for further measurements.

Synthesis of the CdSe USQD-HF-N-LA Nanocomposite. Typically, different amount of 0.0003 M HF-N-LA solution (from 20 to 250 μL, as shown in the inset of Figure 2a, was added to 2 mL of toluene solution containing ultrasmall CdSe QDs. After vigorously stirring for 1 h, 4 mL of isopropanol was added to precipitate the functionalized CdSe QDs. Subsequently, the mixture was centrifuged at 9,500 rpm for 10 min. This process was repeated for three times to ensure that the unattached HF-N-LA molecules were completely removed. The resultant QD-HF-N-LA nanocomposite was then obtained by dissolving the precipitate with toluene.

Characterizations. UV/vis steady-state absorption and emission spectra were recorded with a Hitachi (U-3310) spectrophotometer and an Edinburgh (FS920) fluorimeter, respectively. Experiments of time correlated single photon counting were performed with an Edinburgh FL900 photon-counting system with a hydrogen or nitrogen-filled lamp as the excitation source. Data were analyzed by using the nonlinear least-squares procedure in combination with an iterative convolution method. The emission decay was analyzed by the sum of exponential functions, which allows partial removal of the instrument time broadening and provides a temporal resolution of approximately 300 ps. The shapes and size distributions of the nanocrystals were measured with a JEOL JEM 1230 transmission electron microscope (TEM), and the conventional Formvar coated 200 mesh Cu grids were used.

RESULTS AND DISCUSSION

For the proof of the concept, we select a kind of ultrasmall sized CdSe nanodots, for which its emission band gap is sharp/narrow enough to facilitate the access of white light generation. One well-established CdSe USQD has been reported to emit light at 450 nm.[15] A low temperature synthetic method (at about 100 °C) incorporating hexadecylamine (HDA) and trioctylphosphine (TOP) as surfactants was introduced in that study. It is well-known that mixed surfactants are beneficial for the size and the shape homogeneity. Therefore, we tentatively added trioctylphosphine oxide (TOPO) into the reaction system for the purpose of achieving better control on the size and the shape of QDs as well as improving solubility (see Experimental Section for detail). The absorption and emission spectra of the as-prepared ultrasmall CdSe QDs are shown in Figure 1. The first characteristic excitonic peak at 426 nm and the corresponding emission band maximized at 435 nm firmly support the presence of the CdSe USQDs. Moreover, addition of TOPO greatly improves the solubility of USQDs in nonpolar solvents such as toluene and *n*-hexane in the present case.

In an aim to achieve white-light generation (an ideal CIE value of (0.33, 0.33), the CIE coordinates are constructed by Commission International de l′Eclairage in 1931, in which different colors (emission spectra) can be converted to corresponding coordinates), we then calculated that an ideal countered ligand fluorophore should exhibit emission maximum between 565 and 575 nm to match the CdSe 435 nm emission band. Through judicious design, a new ESIPT molecule composed of flavones

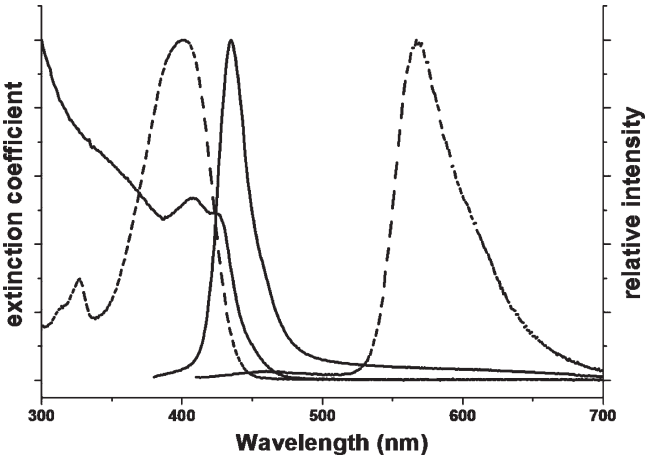

Figure 1. Absorption and emission spectra of ultrasmall CdSe quantum dots (solid line) and HF-N-LA molecules (dashed line).

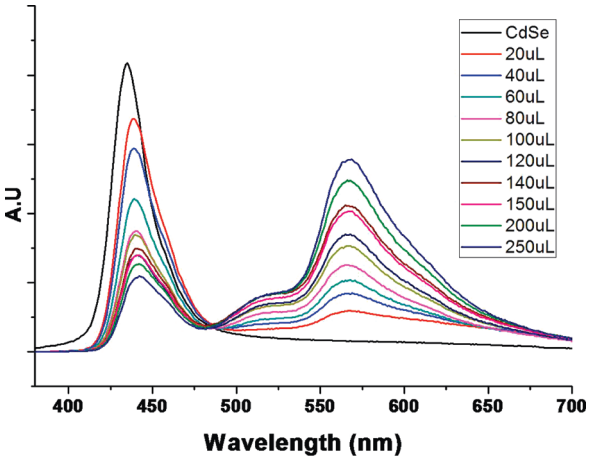

Figure 2. Emission spectra of ultrasmall CdSe QDs by HF-N-L nanocomposites by combining different concentrations of HF-N-LA solutions with fixed amounts of USQDs.

derivatives, namely 5-(1,2-dithiolan-3-yl) -*N*-(2-{[4-(3-hydroxy-4-oxo-4H-chromen-2-yl)phenyl] (methyl)amino}--ethyl)pentanamide (HF-N-LA, see Scheme 1) was synthesized to meet the above-mentioned criterion. The synthetic route and the procedures of HF-N-LA are elaborated in Scheme 1A and the Experimental Section, respectively. The corresponding absorption and the emission spectra of HF-N-LA in toluene are depicted in Figure 1. HF-N-LA exhibits the lowest lying (S_0-S_1) absorption peak wavelength at ~400 nm with tail extending to ~450 nm, which overlaps well with the band-edge absorption of ultrasmall CdSe QDs. Upon excitation, an enormously red-shifted emission maximized at 567 nm is observed (see Figure 1). The Stokes shift between the absorption and the emission peaks is calculated to be as large as 8000 cm^{-1}, signifying the occurrence of ESIPT for HF-N-LA shown in Scheme 1B. No normal emission band can be resolved from the steady state measurement, indicating that the rate of ESIPT must be ultrafast. This observation is also supported by the <1 ps rise time of the 567 nm proton-transfer tautomer emission in cyclohexane in our fluorescence up-conversion experiment (not shown here). This special photophysical feature provides brightening perspective for generating pure white color emission upon incorporating CdSe QDs.

Amid producing white emissive nanocomposite, one ought to determine the extinction coefficient (ε) for both HF-N-LA and ultrasmall CdSe QDs, which is essential for proper combination of QDs and HF-N-LA molecules. According to the Lambert−Beer's law, extinction coefficient of HF-N-LA was calculated to be 2.72×10^4 (cm^{-1} M^{-1}) at 400 nm (see Figure 1). Estimation of the extinction coefficient of ultrasmall CdSe QDs was carried out by using methods established by Mulvaney's group, and the ε value was estimated to be 1.55×10^5 (cm^{-1} M^{-1}) at 426 nm.[28] Because of the fact that the dependence of extinction coefficient on size of nanocrystal is in between a square and cubic manner, one would deduce that the magic sized quantum dots should have lower ε value than the regular sized ones.[28,29] Moreover, the emission yields for CdSe USQDs and HF-N-LA in toluene were measured to be 0.12 and 0.23, respectively. The combination of absorptivity and emission yield provides us a clue to estimate relative amount for CdSe QDs versus HF-N-LA in the as prepared nanocomposites, that is, the amount of HF-N-LA molecules should be slightly larger than that of CdSe QDs by considering the values of extinction coefficient as well as the emission yield of the two species.

With photophysical parameters provided above, we thus synthesized the HF-N-LA incorporated CdSe USQDs by anchoring HF-N-LA onto CdSe QDs with various stoichiometry. The resulting nanocomposite was precipitated, followed by isolation and then redispersion in toluene for further measurements (see Experimental Section). Figure 2 shows the emission spectra of the as prepared nanocomposite as a function of HF-N-LA stoichiometry. The absorption spectral feature is well fitted by the combination of ultrasmall CdSe QDs and HF-N-LA spectra in various ratios (not shown here), indicating the lack of interaction between CdSe and the anchored HF-N-LA in the ground state. For simplicity, assuming equal size of all as prepared CdSe USQDs and homogeneous distribution of HF-N-LA onto each ultrasmall QDs, the molar ratios for CdSe QDs versus HF-N-LA in each composite can thus be deduced from convolution of the absorption spectrum in terms of absorptivity and the corresponding spectral features for each individual fluorophore; the molar ratios of HF-N-LA: ultrasmall CdSe QDs for each nanocomposite are listed in Table 1.

In Figure 2, upon excitation at 365 nm, which is chosen for the purpose of visualization of emission color using commercial UV lamp (vide infra), the emission of the prepared nanocomposite consists of three bands maximized at 440 nm, 520 nm (a shoulder), and 567 nm, among which the emission band with maxima at 440 and 567 nm are identical with those of individual ultrasmall CdSe QDs and HF-N-LA, respectively. Upon increase of anchoring HF-N-LA, the 567 nm proton-transfer emission gradually increases (c.f. 440 nm CdSe emission), showing a good linear proportionality as a function of stoichiometric changes (vide infra).

Lifetime studies were also carried out to examine if there is any interaction between ultrasmall CdSe QDs and the anchored HF-N-LA, giving rise to energy transfer and electron transfer, etc. that quench the emission. As listed in Table 1, emission lifetimes of CdSe USQDs (monitored at 440 nm) and HF-N-LA (monitored at 567 nm) are all within 2.4−2.7 ns and 1.1−1.3 ns, respectively, which, within experimental error, are identical with each individual fluorophore (USQD: 2.65 ns, HF-N-LA: 1.13 ns). The lack of excited-state interaction between CdSe and HF-N-LA is thus well-established.

Table 1. Estimated Molar Ratio of HF-N-LA/CdSe with Respect to the Amount of HF-N-LA Solution (μL) Added into the Ultrasmall CdSe QDs (3 mL) System, And the Fluorescence Lifetime of Each Nanocomposite Monitored at 440 and 567 nm under Excitation of 365 nm

		lifetime[a] (ns)	
addition of HF-N-LA (μL)	HF-N-LA/CdSe molar ratio	440 nm	567 nm
20	0.70	2.48	1.16
40	1.32	2.65	1.33
60	2.17	2.54	1.25
80	3.03	2.60	1.15
100	3.45	2.41	1.26
120	3.71	2.69	1.36
140	3.87	2.57	1.15
150	4.04	2.48	1.27
200	4.45	2.50	1.31
250	4.81	2.43	1.25

[a] The lifetime data of as-prepared ultrasmall CdSe QDs (monitored at 440 nm) and HF-N-LA (monitored at 567 nm) are 2.65 and 1.23 ns, respectively.

Scheme 2. Qualitative Illustration of the White Generation via Anchoring HF-N-LA Molecules onto Surface of the Ultrasmall CdSe QDs[a]

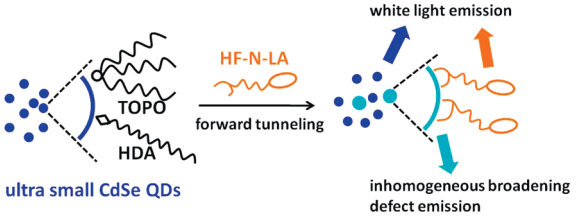

[a] Inhomogeneous broadening as well as defect emission observed in emission spectra are induced by forward tunneling[26] of the USQDs during the replacement of capping molecules.

In addition to the linear tunability for ultrasmall CdSe QDs versus HF-N-LA emission, however, attention has to be drawn here in that a small but non-negligible emission band at ~520 nm gradually appeared amid encapsulating USQDs by HF-N-LA via its dithiol functional groups (see Figure 2). Upon monitoring at the 520 nm emission band, its lifetime was measured to be as long as 10.5 ns. The simplest explanation could be the formation of QD aggregates (fusion) already in the starting material. The possibility of this proposed mechanism is slim due to the following reasons. First, since no additional band was observed in the absorption spectrum, our explanation prone to the growth of certain defect emission during dithiol functionalization. Moreover, we also noted a slight shift from 435 to 440 nm and an asymmetric-like broadening at longer-wavelength side of the blue emission peak shown in Figure 2 during the transformation (The fwhm of the blue emission peak increases from 24 to 35 nm after the anchoring of the HF-N-LA molecules). We therefore provide a plausible explanation by considering the special property of the ultrasmall quantum dots, namely the mechanism of forward tunneling.

It has been reported that ultrasmall QDs would undergo a discontinuous change of particle size from ultrasmall to several

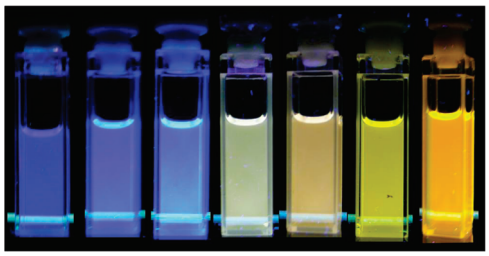

Figure 3. Photographs of nanocomposites with different stoichiometric ratio between HF-N-LA molecules and ultrasmall CdSe QDs, which reveal that the color of nanocomposites could be tuned from blue to yellow.

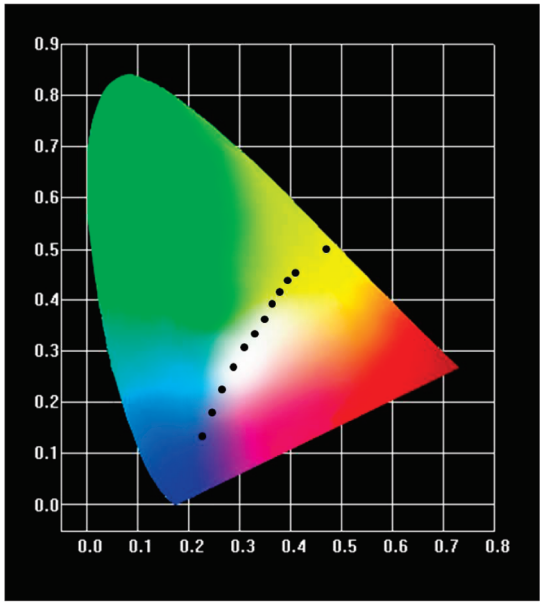

Figure 4. Corresponding CIE coordinates derived from spectra in Figure 2, which shows nearly linear trend of color evolution. Note that the points near (0.2, 0.1) and (0.5, 0.5) are the coordinates of as-prepared ultrasmall CdSe QDs and HF-N-LA molecules, respectively.

nanometers (regular QDs) once the parameters of the surrounding media, such as temperature and/or types of surface ligands, are varied.[30] This forward tunneling of CdSe USQDs to regular QDs could be conducted with the above-described experimental observations in the present system. As shown in scheme 2, briefly, as the HF-N-LA molecules enter into CdSe solution, dithiol functional groups could attach onto surface of ultrasmall QDs by replacing the original surfactants such as TOPO and HDA.[31] During ligand exchange, because of fluctuation of the balance between nanocrystals and surfactants caused by occurrence of −SH ligands, forward tunneling might take place. Newly formed regular QDs with the larger particle size thus induce inhomogeneous broadening of the emission peak around 440 nm.

The 520 nm shoulder in emission spectra of HF-N-LA-ultrasmall QD nanocomposites could therefore be ascribed to the defect emission of larger-sized CdSe QDs, which is commonly seen in emission spectra of regular QDs.[32,33] The growth of 520 nm shoulder accompanied by inhomogeneous broadening in the emission of ultrasmall CdSe QDs implies the transformation of USQDs to regular QDs through forward

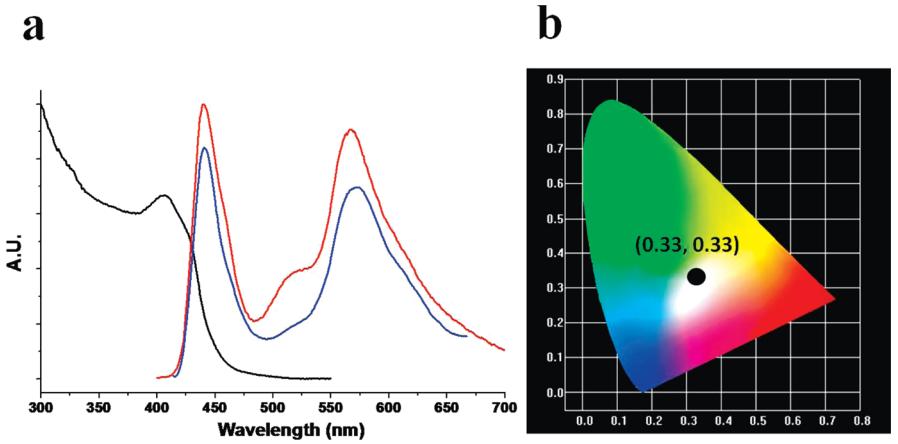

Figure 5. (a) Absorption (black line) and emission spectra (red line) of white light emissive CdSe-HF-N-LA nanocomposites in toluene, and the emission spectrum (blue line) of the nanocomposite−PMMA film. (b) CIE coordinate derived from emission spectrum in a (red line), which clearly shows a pure white emission with a coordinate of (0.33, 0.33).

tunneling. Results of the transmission electron microscope (TEM) of ultrasmall CdSe QDs before and after anchoring HF-N-LA molecules are shown in Figure S1a and S1b in the Supporting Information, respectively. After addition of ESIPT molecules, the particle size of the nanocrystals became slightly larger, and certain disorder in the particle size distribution was observed, further supporting the above statements regarding forward tunneling of the ultrasmall CdSe QDs. On the other hand, though pending resolution, traces of larger CdSe nanoparticles might also be responsible for the 520 nm shoulder. Moreover, a controlled experiment was performed by adding hexadecanethiol into the ultrasmall CdSe QDs solution; the resultant emission spectra are then shown in Figure S2 of the Supporting Information. Obviously, upon introducing thiol molecules, peak shift, inhomogeneous broadening and defect emission were also monitored. Further addition of hexadecanethiol would cause irreversible aggregates of nanocrystals, which are insoluble in toluene. We have made attempts by using different separation techniques to separate any possible regular QDs that give 520 nm emission from the CdSe USQD-HF-N-LA nanocomposites but failed, possibly due to their small difference in size and weight. Nevertheless, the presence of regular CdSe QDs must be rather small in percentage (but with high emission yield) because it has negligible contribution, according to the convolution result, to the observed absorption spectra of the as prepared nanocomposite. Note that the extinction coefficient of regular QDs is larger than the ultrasmall QDs that possess a shape in between a square and a cubic manner.[28,29]

Despite the fact that the presence of 520 nm defect emission band causes a small interference of the net emission color, via varying the HF-N-LA: ultrasmall CdSe QD molar ratio, the color appearance of the USQD-HF-N-LA nanocomposites can be greatly tuned all the way from blue down to yellow-orange, shown in Figure 3. More obviously, the CIE coordinates also reveal linear dependence of the color changes (see Figure 4). The desired color could be produced by applying the lever principle if the linear dependence exists upon mixing two different kinds of colors. This inspiring phenomenon further enriches the feasibility of the as-prepared nanocomposites since the linear trend of color evolution is of immense importance in designing LEDs. It is worth to note that the color tunability is independent of the starting point. In other words, if we reversely add different amount of ultrasmall CdSe QDs into the solution containing fixed amounts of HF-N-LA, the linear trend of color change should still be preserved, as shown in Figure S3 in the Supporting Information, implying that the combination of USQDs and ESIPT molecules here provides a practical route toward generating diverse range of colors, including white color. In the fabrication of white light emitting diodes by mixing two or three kinds of materials, multiple sets of driving chips inside one LED are commonly used; hence the complexity and inhomogeneity may arise because of different characteristics of light emitting species. Alternatively, in this approach, a single nanocomposite offers its advantage in that tuning color is facile via ligand chromophore conjugated to the ultrasmall QDs, covering a designated range of emission with good homogeneity.

As a result, an authentic white emission with (0.33, 0.33) coordinate on CIE graph (color rendering index: 70) can be achieved when the stoichiometry for HF-N-LA: CdSe USQDs is approximately around 3 and 4, as shown in Figure 5. This value is reasonable simply by glancing at the calculated extinction coefficient as well as the emission yield of the two species. The ε of the ultrasmall CdSe QDs is about six times larger than that of HF-N-LA at each peak wavelength. On the other hand, the emission yield of CdSe USQDs is about half of that of HF-N-LA molecules. Therefore, in order to achieve white light generation, number of HF-N-LA should exceed that of the ultrasmall CdSe QDs at least 2−3 times in each composite. During the anchoring process, regular QDs are inevitably produced by forward tunneling mechanism. The presence of these larger sized QDs induces a slightly inhomogeneous broadening and hence a shift of the blue emissive peak. The as-produced CdSe USQDs band edge emission and HF-N-LA proton-transfer tautomer emission, together with in a slight 520 nm defect emission that is utilized to increase the color rendering index.

To firmly demonstrate the feasibility of the as-prepared white emitting nanocomposites, we then blend 10 mg of the CdSe USQD-HF-N-LA with 1 g of poly(methylmethacrylate) (PMMA, Aldrich, M_w = 350 000) powder in 2 mL chloroform. After thorough mixing, the mixture with high viscosity is allowed to undergo spin coating process with 1000 rpm speed. Emission spectrum of the film is then shown in Figure 5a (blue line), which exhibits a similar feature with that in solution phase (red line). The corresponding CIE coordinate of the film is almost the same as that in Figure 5b. Also, the fluorescence lifetime of the as

prepared nanocomposite film monitored at 440 and 567 nm under 365 nm excitation are 2.51 and 1.30 ns, respectively. The consistence of emission spectrum and fluorescence lifetime between samples in solution phase and solid state implies that the nanocomposite is stable through the process of fabricating solid film, further revealing the potential of the hybrid nanocomposite in application. As for the photostability, the emission of USQD-HF-N-LA nanocomposite is rather stable. For the application in PMMA, the intensity as well as the emission ratio remained unchanged after a period of ~10 h irradiation using 365 nm commercial UV-lamp (for TLC). Furthermore, even under the exposure of ambient condition for several weeks, the emission spectrum of the white light is almost the same. Note that the intensity of 520 nm shoulder is lowered in solid state, indicating that defect emission could be quenched in solid phase. The white emissive CdSe USQD-HF-N-LA nanocomposite reported in this study is therefore proven to be an ideal nanomaterial suited for the white-light generation and solid-state lighting.

CONCLUSIONS

In summary, via anchoring the designated ESIPT molecules such as HF-N-LA onto ultrasmall CdSe QDs, fascinating white light emission with CIE coordinate of (0.33, 0.33) as well as linear color tunability can be achieved in one single nanocomposite. Material combination through this facile protocol could thus facilitate a general approach in producing panchromatic light emitting nanocrystals, which would serve as a promising material in the field of light emitting diodes. Furthermore, incorporation of ultrasmall CdSe QDs renders the smaller particle size of the prepared nanocomposites and less amount of HF-N-LA molecules required for white light generation. In addition to LEDs, it is also of great interest to combine these ultrasmall sized nanocomposites with metal organic framework (MOF) and mesoporous materials for further bioimaging as well as biomedical applications. For example, the as prepared nanocomposites could serve as multicolor, ratiometric fluorescence probes for detecting polarity as well as hydrogen bonding in micelles and phospholipid membranes of biosystems.[34−36] Focus of this issue is currently in progress.

ASSOCIATED CONTENT

Supporting Information. TEM images of the ultrasmall CdSe QDs and nanocomposites. Resultant emission spectra of the controlled experiment. Emission spectra and the corresponding CIE coordinate of the nanocomposites produced by adding the ultrasmall CdSe QDs into HF-N-LA solution. This material is available free of charge via the Internet at http://pubs.acs.org.

AUTHOR INFORMATION

Corresponding Author

*E-mail: chop@ntu.edu.tw (P-T.C.); 081579@mail.fju.edu.tw (C.-C.K); chenct@ntu.edu.tw (C.-T.C.).

ACKNOWLEDGMENT

We thank National Science Council, Taiwan, for the generous support.

REFERENCES

(1) Zukauskas, A.; Shur, M. S.; Gaska, R. *Introduction to Solid State Lighting*; Wiley, New York, 2002.
(2) Landau, S.; Erion, J. *Nat. Photon.* **2007**, *1*, 31.
(3) Ziegler, J.; Xu, S.; Kucur, E.; Meister, F.; Batentschuk, M.; Gindele, F.; Nann, T. *Adv. Mater.* **2008**, *20*, 4068.
(4) Dai, Q.; Duty, C. E.; Hu, M. Z. *Small* **2010**, *6*, 1577.
(5) Jang, E.; Jun, S.; Jang, H.; Lim, J.; Kim, B.; Kim, Y. *Adv. Mater.* **2010**, *22*, 3076.
(6) Lita, A.; Washington, A. L., II; van de Burgt, L.; Strouse, G. F.; Stiegman, A. E. *Adv. Mater.* **2010**, *22*, 3987.
(7) Alivisatos, A. P. *Science* **1996**, *271*, 933.
(8) Coe-Sullivan, S.; Woo, W. K.; Bawendi, M. G.; Bulovic, V. *Nature* **2002**, *420*, 800.
(9) Medintz, I.; Uyeda, H. T.; Goldman, E.; Mattoussi, H. *Nat. Mater.* **2005**, *4*, 435.
(10) Huynh, W. U.; Dittmer, J. J.; Alivisatos, A. P. *Science* **2002**, *295*, 2425.
(11) Plass, R.; Pelet, S.; Krueger, J.; Gratzel, M. *J. Phys. Chem. B* **2003**, *106*, 7578.
(12) Ouyang, J.; Zaman, M. B.; Yan, F. J.; Johnston, D.; Li, G.; Wu, X.; Leek, D.; Ratcliffe, C. I.; Ripmeester, J. A.; Yu, K. *J. Phys. Chem. C* **2008**, *112*, 13805.
(13) Evans, C. M.; Guo, L.; Peterson, J. J.; Maccagnano-Zacher, S.; Todd, D. K. *Nano Lett.* **2008**, *8*, 2896.
(14) Kucur, E.; Ziegler, J.; Nann, T. *Small* **2008**, *4*, 883.
(15) Riehle, F. S.; Bienert, R.; Thomann, R.; Urban, G. A.; Kruger, M. *Nano Lett.* **2009**, *9*, 514.
(16) Yu, K.; Hu, M. Z.; Wang, R.; Piolet, M. L.; Frotey, M.; Zaman, M. B.; Wu, X.; Leek, D. M.; Tao, Y.; Wilkinson, D.; Li, C. *J. Phys. Chem. C* **2010**, *114*, 3329.
(17) Clapp, A. R.; Medintz, I. L.; Mauro, J. M.; Fisher, B. R.; Bawendi, M. G.; Mattoussi, H. *J. Am. Chem. Soc.* **2004**, *126*, 301.
(18) Clapp, A. R.; Medintz, I. L.; Uyeda, H. T.; Fisher, B. R.; Goldman, E. R.; Bawendi, M. G.; Mattoussi, H. *J. Am. Chem. Soc.* **2005**, *127*, 18212.
(19) Zhang, Q.; Atay, T.; Tischler, J. R.; Bradley, M. S.; Bulovic, V.; Nurmikko, A. V. *Nat. Nanotechnol.* **2007**, *2*, 555.
(20) Chen, K. Y.; Hsieh, C. C.; Cheng, Y. M.; Lai, C. H.; Chou, P. T. *Chem. Commun.* **2006**, 4395.
(21) Park, S.; Kwon, J. E.; Kim, S. H.; Seo, J.; Chung, K.; Park, S. Y.; Jang, D. J.; Medina, B. M.; Giershner, J.; Park, S. Y. *J. Am. Chem. Soc.* **2009**, *131*, 14043.
(22) Shono, H.; Ohkawa, T.; Tomoda, H.; Mutai, T.; Araki, K. *ACS Appl. Mater. Inter.* **2011**, *3*, 654.
(23) Hsieh, C. C.; Jiang, C. M.; Chou, P. T. *Acc. Chem. Res.* **2010**, *43*, 1364.
(24) Hsieh, C. C.; Chou, P. T.; Shih, C. W.; Chuang, W. T.; Chung, M. W.; Lee, J.; Joo, T. *J. Am. Chem. Soc.* **2011**, *133*, 2932–2943.
(25) Mutai, T.; Tomoda, H.; Ohkawa, T.; Yabe, Y.; Araki, K. *Angew. Chem., Int. Ed.* **2008**, *47*, 9522.
(26) Zhang, X.; Xiao, Y.; Qian, X. *Org. Lett.* **2008**, *10*, 29.
(27) Clerici, A.; Ghilardi, A.; Pastori, N.; Punta, C.; Porta, O. *Org. Lett.* **2008**, *10*, 5063.
(28) Jasieniak, J.; Smith, L.; Embden, J.; Mulvaney, P.; Califano, M. *J. Phys. Chem. C* **2009**, *113*, 19468.
(29) Yu, W. W.; Qu, L.; Guo, W.; Peng, X. *Chem. Mater.* **2003**, *15*, 2854.
(30) Yu, Q.; Liu, C. Y. *J. Phys. Chem. C* **2009**, *113*, 12766.
(31) Hsieh, J. M.; Ho, M. L.; Wu, P. W.; Chou, P. T. *Chem. Commun.* **2006**, 615.
(32) Qu, L.; Peng, Z. A.; Peng, X. *Nano Lett.* **2001**, *1*, 333.
(33) Peng, Z. A.; Peng, X. *J. Am. Chem. Soc.* **2001**, *123*, 183.
(34) Klymchenko, A. S.; Demchenko, A. P. *Langmuir* **2002**, *18*, 5637.
(35) Klymchenko, A. S.; Duportail, G.; Mely, Y.; Demchenko, A. P. *Proc. Natl. Acad. Sci. USA* **2003**, *100*, 11219.
(36) Shynkar, V. V.; Klymchenko, A. S.; Piemont, E.; Demchenko, A. P.; Mely, Y. *J. Phys. Chem. A* **2004**, *108*, 8151.